Hot Jupiter Magnetospheres

George B. Trammell, Phil Arras, and Zhi-Yun Li

Department of Astronomy, University of Virginia, Charlottesville VA USA

Introduction/Motivation

Hot Jupiters orbit their stars at distances $D \sim 0.1$ AU and are subjected to $\sim 10^4$ times larger stellar irradiation than solar system gas giants. EUV heating can result in temperatures $T \sim 10^4$ K, increasing the atmospheric scale height. Thermal pressure gradients, complemented by the stellar tide and centrifugal forces may drive an outflow and lead to mass/angular momentum loss from the planet. This region of the atmosphere, important for determining atmospheric escape, is observable through transmission spectroscopy when the planet passes in front of its host star.

Transit depths for the hot Jupiter HD 209458b observed in Lyα by [7,8,4] indicate H I absorption at several planetary radii, comparable to the size of the planet's Roche Lobe. Similar results have been seen for Na I [2], O I and C II [8]. The H I transit depth has been interpreted to indicate atmospheric escape, with heavier C and O atoms entrained in the outflow.

However, an ionized upper atmosphere with a Jupiter-size magnetic field will be "magnetically confined" near the equator, restricting the range of latitudes over which escape occurs. Although field strengths for exoplanets are currently unconstrained by observation, recent dynamo theories suggest hot Jupiters may have strong fields [3], we argue perhaps even stronger than that of Jupiter. Therefore a large magnetosphere may surround the planet, even beyond the Roche-Lobe distance. Our models [6] address this strong field limit.

Structure of the Upper Atmosphere

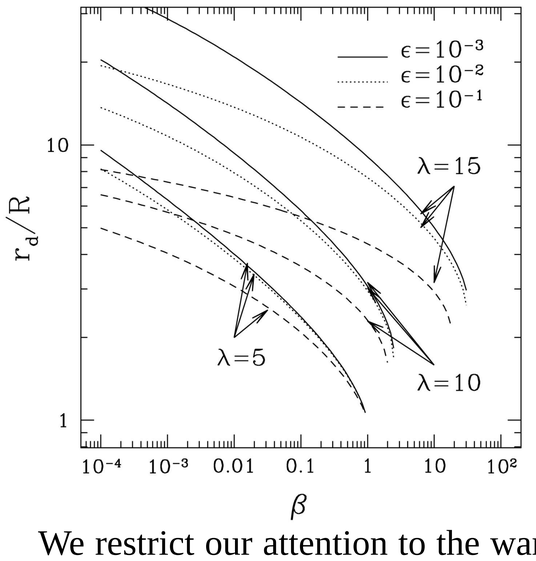

Fig 1. --- The size of the closed magnetic field line region ("dead-zone", r_d) relative to a planetary radius (R), as functions of parameters defined at the substellar base of the atmosphere for $\lambda = GM/(Ra^2)$, $\varepsilon = (\Omega R/a)^2$, and $\beta = P_{gas}/P_{mag}$, for a planet with mass M and radius R, isothermal sound speed a, and orbital frequency Ω. A larger value of λ (ε) implies density decreases outward faster (slower); the dead-zone size increases (decreases) for larger λ (ε). For a fiducial case with $\varepsilon = 10^{-3}$, $\lambda = 10$, and $\beta = 10^{-2}$, the more rapid decrease of magnetic pressure with radius implies equality with gas pressure at $r_d/R \sim 10$. Increasing ε moves the cusp radius r_d inward. Increasing the magnetic field moves r_d outward (i.e., smaller β) (from Fig. 5 of [6]).

We restrict our attention to the warm H I/H II layers heated by incoming EUV photons. Theory of thermal-magneto-centrifugally driven MHD winds [e.g., 5], gives guidance for computing the density/velocity structure of a rotating one-fluid isothermal atmosphere. A choice of escape speed relative to sound speed (λ), ratio of gas pressure to magnetic pressure (β), and stellar tide strength (ε) will determine the regions where ram pressure can open planetary magnetic field lines (Fig. 1), where mass/angular momentum loss can occur. Regions of closed field lines ($r < r_d$) will contain static gas confined by the magnetic field (the equatorial "dead zone"). A sufficiently strong stellar tide can create a second "polar dead-zone" near the magnetic poles, due to the large potential barrier.

Global Models: Transit Signal for Ly α

A photoionization model is used to compute the distribution of neutral H column density N_H from the density/velocity distributions. Fig. 2 shows maps of N_H as viewed at transit for a range of model parameters that determine the three-zone morphology: (1) the equatorial and (2) polar dead zones, and (3) the wind zone. Lyα transmission spectra, showing the fractional flux decrease ($1\text{-}T_\nu$) versus wavelength, are computed using the column density map (Fig. 3).

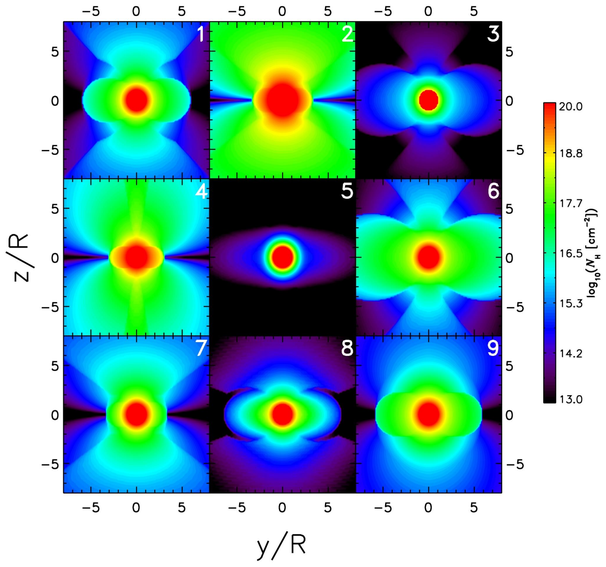

Fig 2. --- Contours of neutral H column density N_H [cm^{-2}] vs. impact parameter as observed during transit for M = 0.7 M_{Jup}, R = 1.4 R_{Jup}, while varying the gas pressure at the substellar point P, sound speed a, magnetic field strength B_0, and orbital distance D. The fiducial case (model 1) displays the equatorial and polar dead zones (DZs), with the mid-latitude wind zone (WZ) having lower N_H. Model 2 (3) has larger (smaller) P, which decreases (increases) the size of the DZ, as well as scaling up (down) the density in the WZ. Model 4 (5) has larger (smaller) a, leading to larger (smaller) density at a fixed impact parameter, while increasing (decreasing) the size of the DZ. Model 6 (7) has larger (smaller) B_0, which increases (decreases) the size of the DZ. Model 8 (9) has larger (smaller) D. Larger tide is more effective at shutting off a wind at the poles, but leads to a smaller equatorial DZ (from Fig. 14 of [6]).

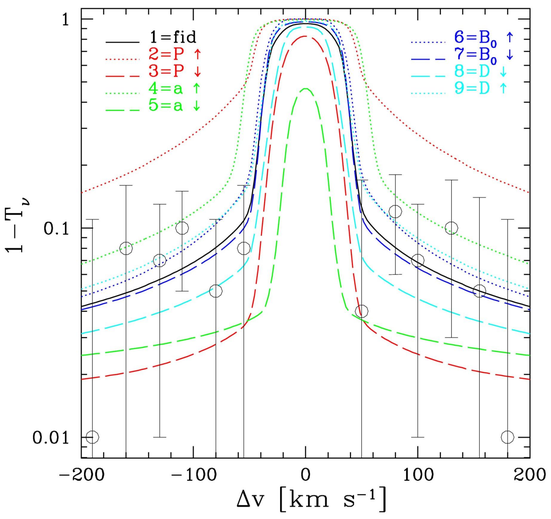

Fig 3. --- Fractional flux decrease vs. frequency in velocity units [km s^{-1}] for HD 209458b. The different color curves correspond to spectrum computed from the 9 models of Fig. 2, with a variation of the single parameter as indicated in the top of the plot. The data points with error bars are from Fig. 6 of [1]. The entire planetary atmosphere is optically thick near line center and there is near complete absorption. Moving away from line center through the Doppler core, eventually the absorption cross-section becomes small enough for the atmosphere to become optically thin and $1\text{-}T_\nu$ decreases rapidly. The curves level out in the damping wings at $\Delta v \sim 50$ km s^{-1} where optical depth τ_ν occurs deeper in the atmosphere (from Fig. 16 of [6]).

Summary

The goal was to simultaneously include the dynamical influence of a planetary magnetic field and a stellar tidal force on the structure of a hot Jupiter upper atmosphere. For field strengths comparable to Jupiter (B_0 = 8.6 G), an equatorial region of static, magnetically-confined gas can dominate the transit depth. Hence the existence of neutral hydrogen beyond the planet's Hill radius does not necessarily imply mass loss.

References

[1] Ben-Jaffel L., 2008, ApJ, 688, 1352
[2] Charbonneau D., et al. 2002, ApJ, 568, 377
[3] Christensen U.R., et al. 2009, Nature, 457, 167
[4] Ehrenreich D., et al. 2008, A&A, 483, 933
[5] Spruit H.C. 1996, arXiv:astro-ph/9602022
[6] Trammell G.B., Arras P., Li Zhi-Yun, 2011, ApJ, 728, 152
[7] Vidal-Madjar A., et al. 2003, Nature, 422, 143
[8] Vidal-Madjar A., et al. 2004, ApJ, 604, L69